separations

MDPI

Article

Removal of Indium Ions from Aqueous Solutions Using Hydroxyapatite and Its Two Modifications

Inga Zinicovscaia [1,2,*], Nikita Yushin [1], Doina Humelnicu [3], Maria Ignat [3], Ionel Humelnicu [3], Dmitrii Grozdov [1] and Tatyana Vershinina [1]

[1] Department of Nuclear Physics, Joint Institute for Nuclear Research, Joliot-Curie Str., 6, 1419890 Dubna, Russia; ynik_62@mail.ru (N.Y.); dsgrozdov@rambler.ru (D.G.); vershinina@nf.jinr.ru (T.V.)
[2] Department of Nuclear Physics, Horia Hulubei National Institute for R&D in Physics and Nuclear Engineering, 30 Reactorului Str. MG-6, 077125 Magurele, Romania
[3] Faculty of Chemistry, Alexandru Ioan Cuza University of Iasi, Bld. Carol I, 11, 700506 Iasi, Romania; doinah@uaic.ro (D.H.); maria.ignat@uaic.ro (M.I.); ionel@uaic.ro (I.H.)
* Correspondence: zinikovskaia@mail.ru; Tel.: +7-496-21-65609

Abstract: Hydroxyapatite (HAP) coupled with its two modifications HAP P123 and HAP F127 were applied for indium removal from aqueous solutions. Adsorbents' abilities to remove indium ions were assessed in relation to pH, time of contact, indium concentration, temperature, and presence of co-existing ions. Adsorption was discovered to be pH-dependent for all sorbents, with maximum indium ion removal at pH 4.0. Both the Langmuir and the Freundlich isotherm models were used to explain the experimental results. For all adsorbents, the Freundlich isotherm provided a better description of the equilibrium of the sorption. The sorption capacity computed from the Langmuir model changed from 10,799 mg/g for HAP F127 to 11071 mg/g for HAP. A number of models were used to describe the adsorption's kinetics. The adsorption of indium on HAP was better described by the pseudo-second-order model, on HAP P123 by the pseudo-first-order model, and on HAP F127 by the Elovich model. Thermodynamic parameters showed that indium ions' adsorption onto HAP adsorbents was a feasible, spontaneous, and exothermic process. The effectiveness of indium removal by the examined adsorbents was unaffected by the presence of other metal ions in the solutions. ORCA quantum chemistry software was used to theoretically examine the interactions between the surfaces of adsorbents and the indium ions. High desorption efficiency showed that the applied adsorbents can be used for manifold wastewater treatment.

Keywords: hydroxyapatite; indium removal; recovery; pollution; thermodynamic; adsorption; kinetics; equilibrium

Citation: Zinicovscaia, I.; Yushin, N.; Humelnicu, D.; Ignat, M.; Humelnicu, I.; Grozdov, D.; Vershinina, T. Removal of Indium Ions from Aqueous Solutions Using Hydroxyapatite and Its Two Modifications. *Separations* **2023**, *10*, 401. https://doi.org/10.3390/separations10070401

Academic Editor: Xinhua Qi

Received: 19 June 2023
Revised: 9 July 2023
Accepted: 11 July 2023
Published: 12 July 2023

1. Introduction

Heavy metals are pollutants that are regularly discovered in industrial wastewater. These pollutants are typically produced by a variety of industrial processes, including the mining, electroplating, metal smelting, chemical, and paint industries. The presence of heavy metals beyond acceptable limits can provoke serious health and environmental damage [1–3].

Indium possesses distinct physical and chemical characteristics which determine its wide application in the electronics industry (liquid crystal displays, semiconductor devices, solar cells) [4], for the production of semiconductor devices and alloys, as well as in the nuclear industry [5]. Despite being used extensively, indium is widely dispersed in nature and is only frequently found in small amounts in some ores of zinc, copper, and lead sulfide [5]. In recent years, indium consumption and price have increased rapidly, and consequently, its recovery from wastewater and waste materials can realize its circular exploitation and prevent release in natural water bodies. According to reports, indium's

cytotoxicity and protracted persistence in nature can cause serious harm to the heart, kidney, and liver [3].

Numerous techniques, including ion exchange [5,6], liquid-liquid extraction [7], chemical precipitation [8], electroanalytical methods [9], and adsorption [10,11], have been applied for indium recovery.

Among the mentioned techniques, adsorption represents one of the most suitable methods for indium removal due to its low cost, simplicity, efficiency, and low energy consumption [12–15]. As adsorbents for indium recovery, the following materials were applied: modified solvent-impregnated resins (MSIRs) [16], the ion-imprinted polymer [17], phosphorylated sawdust bead [12], carbon nanotubes [18], chitosan-coated bentonite [13], carboxymethyl chitosan/poly(acrylic acid) [19], layered silicates [20], modified chitin [21], multifunctional alginate [22], and SiO_2@GO-PO_3H_2 composite [23]. Despite the active application of the adsorbents for indium recovery, for the main part of them, low values of the adsorption capacity were achieved [12,13,17]. As a result, current research is concentrated on developing new and effective adsorbents for indium removal from wastewater.

Hydroxyapatite ($Ca_{10}(PO_4)_6(OH)_2$, HAP) is an important adsorbent used for the removal of hazardous pollutants (e.g., heavy metals, dyes) from wastewater [24,25]. This material is easily synthesized on a large scale by using different methods in order to obtain more effective HAP-based sorbents. The morphology and adsorption capacity of HAP are influenced by the type of synthesis procedures. From an economic point of view, hydroxyapatite and its derivatives have developed as appropriate alternative adsorbents for the treatment of wastewater contaminated with heavy metals.

Over the past years, due to its strong adsorption affinity to diverse water pollutants, low water solubility, thermal stability, and ionic exchange capacity, hydroxyapatite has attracted enormous attention for its effectiveness in the removal of heavy metal ions [26,27]. HAP was actively used in several research studies for the removal of various pollutants. The maximum adsorption capacities of HAP reported by Nu'nez et al. [28] for Pb(II), Cd(II), and Cu(II) constituted 265, 64, and 55 mg/g, respectively.

Based on our previous works [29,30], the HAP and its derivative forms were chosen in this study as adsorbents to investigate the recovery of indium (III) from batch solutions. The effect of physico-chemical parameters, such as pH, time of contact, indium concentration, temperature, and presence of co-existing ions on the HAP's adsorption efficiency, were investigated. To comprehend the mechanics of adsorption, different kinetic and equilibrium models were used.

2. Materials and Methods

2.1. Chemicals

All chemicals used to synthesize the adsorbents and the $In_2(SO_4)_3$ used to perform sorption experiments were of analytical grade (Sigma-Aldrich, Darmstadt, Germany).

2.2. Sorbents' Preparation

The procedure presented by Arsad et al. [31] was followed in order to produce hydroxyapatite (HAP). In the first stage, solution of calcium nitrate (0.5 M) was mixed with ethanol (50 mL) and the pH of the mixture was raised to 10. In the second stage, the phosphoric acid (0.3 M) was added to the mixture dropwise. The reaction started at 60 °C for 1 h, and then it continued for the remaining 24 h at room temperature. After the reaction, the suspension was centrifuged for 15 min at 4000 rpm to separate the precipitate, which was then subjected to a 6 h calcination process at 550 °C. Except for the application of Pluronic P123 and Pluronic F127, the sorbents HAP P123 and HAP F127 were prepared according the same procedure.

2.3. Adsorption Experiments

The influence of pH, time of contact, indium concentration, temperature, and co-existing ions on the adsorption capacity of HAP adsorbents was assessed. In all experiments,

except equilibrium studies, the dosage of the sorbent and the volume of the experimental solution were constant: 20 mg and 10 mL, respectively. The pH of the experimental solutions ranged from 2.0 to 6.0 and was changed to the necessary values using 0.1 M NaOH or HCl. The effect of the other parameters was studied at optimal pH values. In the equilibrium studies, the following concentrations of indium were used: 10, 20, 30, 40, 50, 75, 100, 200, and 300 mg/L; pH (4.0), time (1 h), and temperature (22 °C) were kept constant. In kinetic experiments, the parameter which varied was time, and samples were withdrawn at 1, 3, 5, 7, 15, 30, 45, and 60 min. Thermodynamic studies were performed at temperatures ranging 20–50 °C.

Indium in nature is mainly associated with cadmium, zinc, copper, and tin deposits [5,8]. Thus, the effect of copper, tin, cadmium, and zinc on the indium adsorption onto HAP sorbents was studied. Experiments were performed at pH 4.0, temperature 22 °C, and time of contact 60 min. The concentrations of all elements in the system were 10 mg/L.

Adsorption experiments (carried out in triplicate) were performed at constant stirring on a rotary Unimax 1010 shaker (Heidolph, Schwabach, Germany).

Equations (1) and (2) were used to assess the HAP's adsorption capacity and removal efficiency:

$$q = \frac{V(C_i - C_f)}{m} \quad (1)$$

$$R = \frac{C_i - C_f}{C_i} \times 100 \quad (2)$$

where q (adsorption capacity) = mg/g, V (solution volume) = L, C_i and C_f (indium initial and final concentrations) = mg/L, and m (sorbent weight) = g.

2.4. Methods

An ICP-OES PlasmaQuant PQ 9000 Elite spectrometer (Analytik Jena, Jena, Germany) was used to measure the indium concentrations in the initial solutions and following the batch tests. Qualitative Phase Analysis was carried out on an EMPYREAN X-ray diffractometer (PANalytical) using Bragg-Brentano focusing method. Bragg-Brentano (CoKα radiation) was in the angular range 2θ = 20–80° with a step $\Delta\theta$ = 0.026°. The analysis of the obtained data was carried out using the PDF-4 database. The infrared spectra were recorded using a Bruker Alpha Platinum-ATR spectrometer (Bruker Optics, Ettingen, Germany) in the range between 4000 and 400 cm^{-1}.

2.5. Reusability of the Sorbents

Three adsorption/desorption cycles were used with the goal of demonstrating multiple uses of HAP and its modifications. Firstly, adsorption of indium at optimal conditions was carried out, then 0.01 M HCl was as eluted for element. At the end of the first sorption/desorption cycle, adsorbents were washed multiple times with distilled water and the procedure was repeated for the next two cycles.

3. Results and Discussion

Detailed characterization of the applied sorbents using scanning electron microscopy, Fourier-transform infrared spectroscopy, and nitrogen adsorption–desorption analysis is presented in [29,30]. The Ca/P ratio in the HAP sorbent was 1.67. The highest specific surface area of 69.1 ± 0.1 m^2/g was obtained for HAP P123, followed by HAP (47.2 ± 0.1 m^2/g) and HAP F127 (31.7 ± 0.1 m^2/g). As can be seen, the addition of the surfactant F127 led to a decrease in the specific surface area, which is in agreement with [32].

X-ray diffraction analysis (Figure 1) showed that only hydroxyapatite was present in the HAP P123 adsorbent (PDF No. 00-064-0738), while in HAP and HAP F127, β-$Ca_2P_2O_7$ (PDF No. 00-020-0024) and brushite (PDF No. 98-010-9193) were also found.

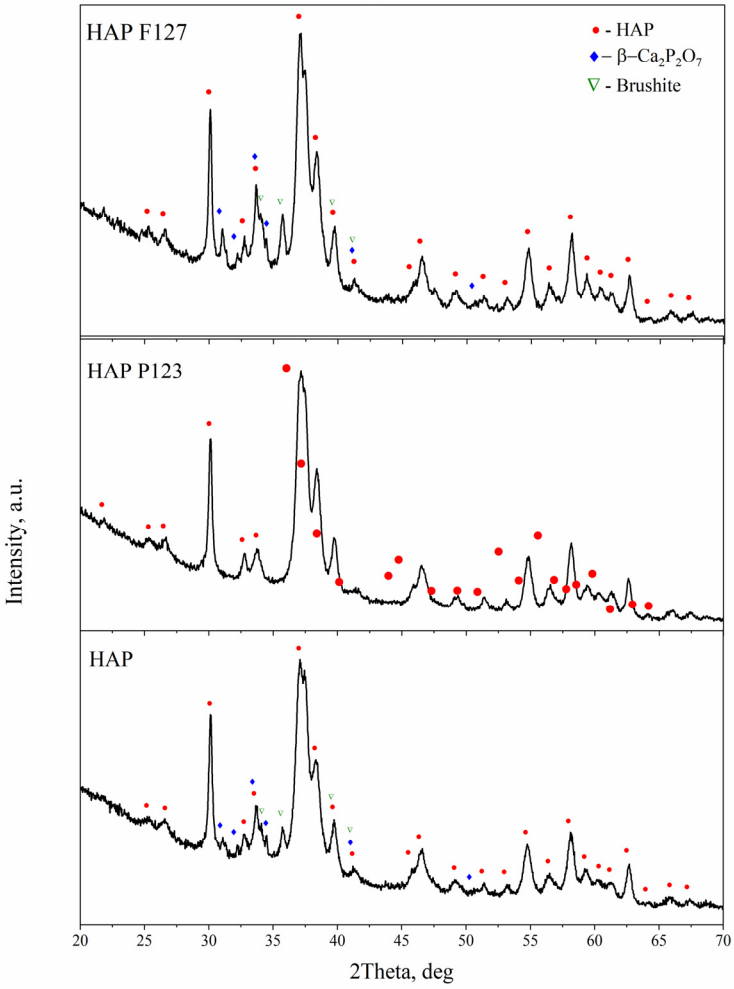

Figure 1. X-ray spectra of the studied adsorbents.

After indium adsorption, the phase composition of the adsorbents did not change. As an example, the X-ray spectra of HAP P123 before and after indium adsorption is illustrated in Figure 2.

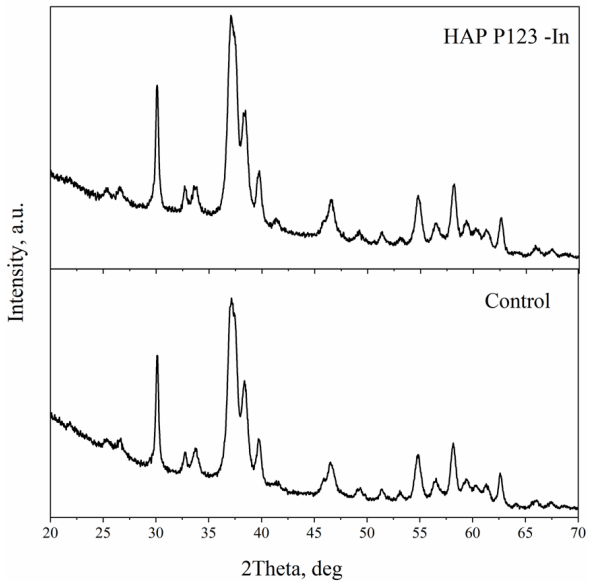

Figure 2. X-ray spectra of HAP P123 before and after indium adsorption.

FTIR analysis was used to assess the involvement of the functional groups in indium removal (Figure 3). The peaks at 1010 and 1015 cm^{-1} observed in the HAP, control, and indium-loaded samples (Figure 3a) were due to the asymmetric stretching vibration of the P–O bond of phosphate PO_4^{3-} groups [33,34]. The bands detected at 600 and 605 cm^{-1} are attributed to the bending vibration of the O–P–O bond of phosphate PO_4^{3-} groups [33]. The weak band at 3300 cm^{-1} is assigned to the O–H stretching vibration of surface P–OH groups [33]. In the FTIR spectrum of HAP loaded with indium, a decrease in the intensity of deformation bands of PO_4^{3-} ions was observed. In the case of HAP P123 and its form loaded with indium (Figure 3b), the peaks at 1005 and 1010 cm^{-1} are also attributed to the asymmetric stretching vibration of the P–O bond of phosphate PO_4^{3-} groups [33,34]. The bands at 680 and 655 cm^{-1} reveal the bending vibration of the O–P–O bond of the phosphate group [33], and the band at 3000 cm^{-1} is assigned to the O–H stretching vibration [33]. In the FTIR spectrum of HAP P123-In, an increase in the intensity of deformation bands of PO_4^{3-} ions was seen. In the spectrum of HAP F127, the same functional groups were observed (Figure 3c). The peaks at 1010 and 1012 cm^{-1} corresponded to the asymmetric stretching vibration of the P–O bond [33,34], that at 690 cm^{-1} was due to the vibration of the O–P–O bond of phosphate groups, and that at 2950 cm^{-1} was assigned to the O–H groups [33]. There, the spectrum of control HAP F127 was very similar with the indium-loaded adsorbent.

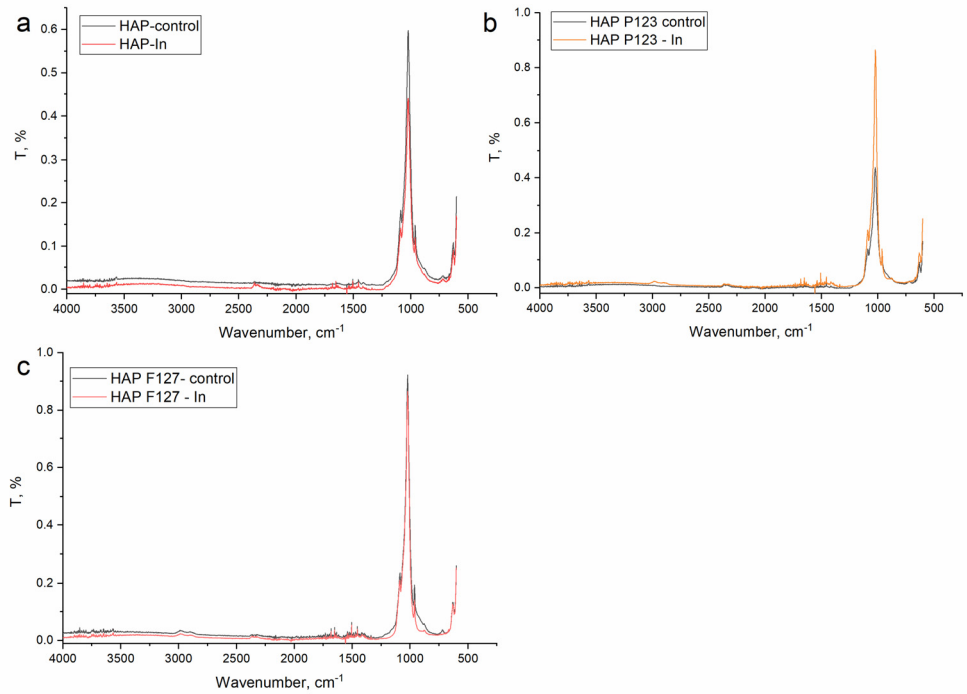

Figure 3. FTIR spectra of adsorbents before and after indium adsorption: (**a**) HAP, (**b**) HAP P123 and (**c**) HAP F127.

The change in intensity of PO_4^{3-} bands can indicate indium ions' interaction with calcium ions and protons via ion-exchange or their coordination with PO_4^{3-} groups [30].

3.1. Effect of pH on Indium Removal by HAP Adsorbents

One of the most crucial variables in the adsorption process is the pH of the solution. In order to avoid indium ions' precipitation, the process of sorption was investigated at a pH below 6.0. As can be followed from Figure 4, at pH 2.0 the effectiveness of indium removal by HAP adsorbents was between 25 and 36%. The low adsorption of indium ions is explained by the presence of the high concentration of H^+ ions and their competition with the indium ions for binding sites [5,29,30]. Maximum adsorption of indium onto HAP of 7.6 mg/g (98.7%)–7.7 mg/g (99.8%) was achieved at pH 3.0–4.0. The same pattern was

obtained for modified adsorbents, with the removal efficiency constituting 99.8% for HAP P123 and 96.7% for HAP F127.

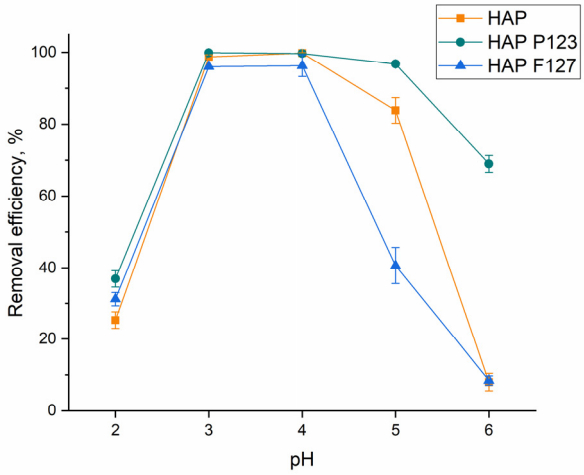

Figure 4. Effect of pH on indium removal by HAP adsorbents.

Indium mainly exists as In^{3+}, $In(OH)^{2+}$, and $In(OH)^{2+}$ species at pH < 4.0, while at higher pH values the formation of $In(OH)_3$ begins [35]. Thus, a drastic decrease in indium removal at a pH higher than 4.0 can be explained by $In(OH)_3$ formation, since the number of OH groups in the solution has increased as a result of using NaOH to adjust the pH. According to Calagui et al. [13], adsorption and precipitation were responsible for indium adsorption onto chitosan-coated bentonite at the pH range 4.0–6.0. In the Chou [36] experiments, it was shown that at pH 5.0 and 6.0, 14–22% of indium ions were removed due to interactions with sodium hydroxide and 50–65% were adsorbed onto spent coffee grounds.

Maximum adsorption of indium ions by poly(vinylphosphonic acid-co-methacrylic acid) microbeads was achieved at pH 6.0 [5], by carbon nanotubes at pH 10 [18], by brown alga *Ascophyllum nodosum* at pH 3.0 [37], and by amino methylene phosphonic acid resin at pH 3.6 [38]. To ensure high removal efficiency, further experiments were carried out at pH 4.0.

3.2. Effect of Time on Indium Removal by HAP Adsorbents and Kinetics of Study

Assessment of the effect of contact time on the sorption efficiency could help researchers to understand the possible mechanisms of the sorption reaction [39]. Figure 5 represents a plot of the indium ions' removal efficiency versus contact time.

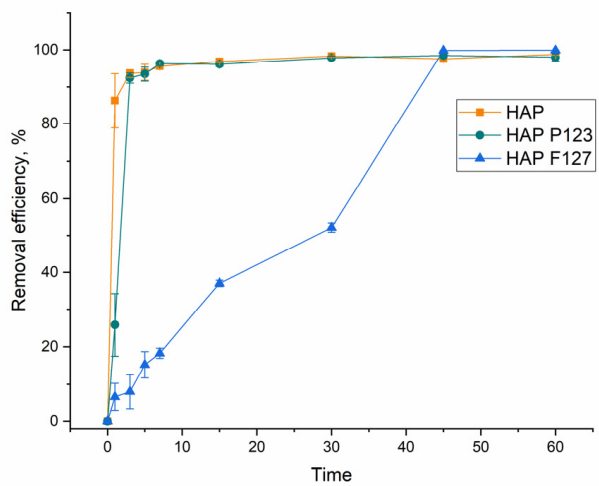

Figure 5. Effect of time on indium removal by HAP adsorbents.

Approximately 86% of the indium ions were removed from the solution during the first minute of the interaction. A Maximum indium removal of 96% was achieved in 7 min and then equilibrium was attained. Even in the first min of HAP P123 interaction with indium, only 26% of ions were removed from the solution; in the next 3 min, the removal increased up to 92% and in 30 min equilibrium was attained. In the case of HAP F127, it took a longer time to achieve maximum indium ions' removal; the removal efficiency of the sorbent increased gradually and equilibrium was reached in 45 min.

The indium adsorption onto HAP and its modifications can be described as a two-step process. The rapid adsorption of indium ions in the first minutes of interaction is explained by the abundance of vacant binding sites on the external surface. The decrease in the removal efficiency with the increase in the contact time is due to the saturation of the external sites, which causes the diffusion of indium ions into the internal surface of the adsorbent [40–42]. The surface modifications can be responsible for the variations in equilibrium times between the adsorbents [41].

In order to gain more information about the mechanism of adsorption, the pseudo-first-order, pseudo-second-order, and Elovich models were applied (Equations (3)–(6)).

The pseudo-first-order model:

$$q_t = q_e \left(1 - e^{-k_1 t}\right) \tag{3}$$

The pseudo-second-order model:

$$q = \frac{q_e^2 k_2 t}{1 + q_e k_2 t} \tag{4}$$

The Elovich model:

$$q_t = \frac{1}{\beta} \ln(1 + \alpha\beta t) \tag{5}$$

where q_t (indium amount adsorbed at instant t) = mg/g; k_1 (the pseudo-first-order rate constant) = 1/min; k_2 (the second-order reaction rate constant) = g/mg·min; and α and β (Elovich model constants) = g/mg·min and g/mg, respectively.

Figure 6 displays the results of the non-linear fitting of the experimental data, and Table 1 lists the kinetic parameters and correlation coefficients.

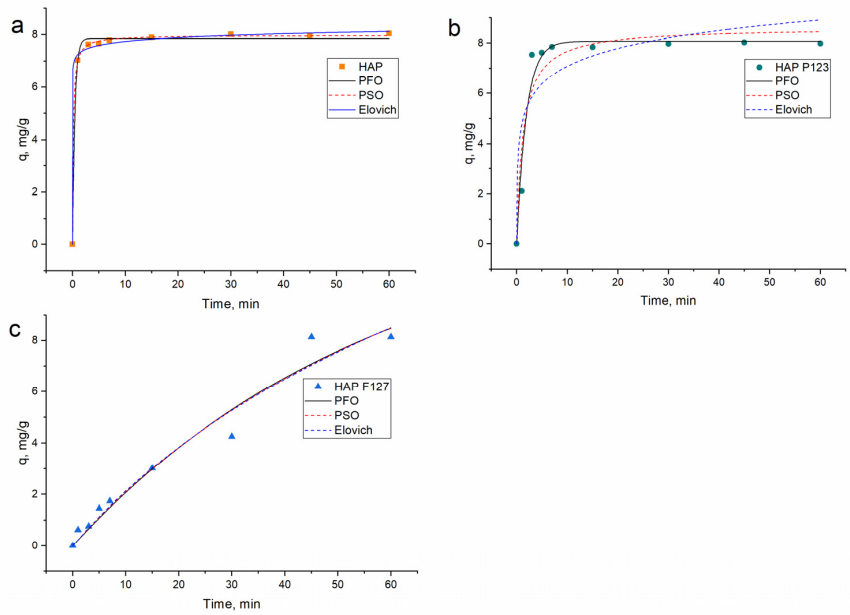

Figure 6. Indium adsorption onto HAP adsorbents described by pseudo-first-order, pseudo-second-order, and Elovich models: (**a**) HAP, (**b**) HAP P123, and (**c**)HAP F127.

Table 1. Kinetic model parameters calculated for HAP and its two modifications.

Sorbent	Kinetics								
	Pseudo-First Order			Pseudo-Second Order			Elovich		
	q_e	k_1	R^2	q_e	k_2	R^2	α	β	R^2
HAP	7.85 ± 0.07	2.24 ± 0.19	0.99	7.98 ± 0.03	0.88 ± 0.07	0.99	1.1E14 ± 6.4	4.67 ± 0.73	0.99
HAP P123	8.06 ± 0.28	0.52 ± 0.09	0.96	8.62 ± 0.54	0.09 ± 0.04	0.914	105.9 ± 24.3	0.98 ± 0.36	0.81
HAP F127	13.32 ± 4.40	0.01 ± 0.008	0.96	21.8 ± 8.7	4.8 ± 0.00	0.96	0.24 ± 0.05	0.11 ± −0.05	0.96

In the case of HAP sorbents, the coefficient of correlation values for all applied models were 0.99. However, the Elovich model, due to the extremally high value of α, can be considered appropriate for the description of experimental values. The adsorption of indium ions on HAP, as determined using the Akaike information criterion (AIC) test, followed a pseudo-second-order model. Moreover, q_e values calculated from the pseudo-second-order model were very close to the experimental values. The use of the pseudo-second-order model led to the conclusion that chemisorption, which is based on the ionic character of binding through the sharing or exchange of electrons between the adsorbent and adsorbate [42], is the rate-limiting stage of indium adsorption [40]. Since indium is present in solution in its cationic form, its adsorption may occur due to ion exchange with calcium ions or surface complex formation with the phosphate groups on the adsorbent [43].

The low R^2 values for the pseudo-first-order and Elovich models demonstrated that the adsorption of indium onto HAP P123 could not be explained by these models. The higher R^2 value for the pseudo-first-order model showed that it was best fitted to the experimental data. The results of the AIC test also confirmed this fact. In the case of HAP F127, the R^2 values for all models were 0.96. However, according to the AIC test, the Elovich model was better suited to describe experimental data. The Elovich model is applicable to explain the heterogeneous chemisorption process [42].

3.3. Effect of Indium Concentrations on Its Removal by HAP Adsorbents and Equilibrium of Study

Figure 7 shows the effect of various indium ion concentrations on HAP and its two modification adsorption capacities.

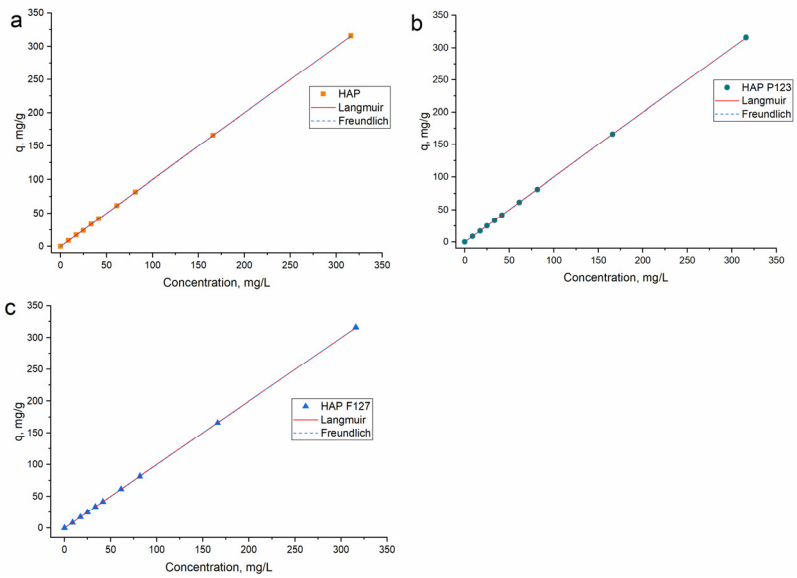

Figure 7. Indium adsorption onto HAP adsorbents described by Langmuir and Freundlich models: (**a**) HAP, (**b**) HAP P123, and (**c**) HAP F127.

The increase in the adsorption capacity of the examined sorbents was linked to the rise in indium content in the solution. For all adsorbents, the adsorption capacity rose from 8.6 to

316 mg/g as the initial concentration increased from 10 to 300 mg/L. A higher driving force in mass transfer operations between the aqueous and solid phases can be used to explain the high adsorption capacity of the adsorbents at high indium concentrations [44,45].

Langmuir (6) and Freundlich (7) adsorption isotherms were applied to describe equilibrium of the adsorption.

$$q_m = \frac{q_m\, bC_e}{1 + bC_e} \tag{6}$$

$$q_m = K_F Ce^{\frac{1}{n}} \tag{7}$$

where C_e (indium concentration at equilibrium) = mg/L; q_m (maximum amount of indium adsorbed) = mg/g; b (Langmuir constant) = L/mg; and K_F and n (Freundlich constants).

The separation factor R_L was calculated using Equation (8).

$$R_L = \frac{1}{1 + bC_i} \tag{8}$$

Adsorption is considered favorable when the R_L value is less than one unit and unfavorable when the R_L value exceeds one unit.

Figure 6 displays the nonlinear fitting of the data, and Table 2 summarizes the R^2 and isotherm parameters.

Table 2. Isotherm model parameters cucullated for HAP and its two modifications.

Sorbent	Isotherms					
	Langmuir			Freundlich		
	q_m	b	R^2	K_F	n	R^2
HAP	11,071 ± 1712	9.04×10^{-6}	0.99	0.98 ± 0.011	0.99 ± 0.002	0.99
HAP P123	11,035 ± 907	9.07×10^{-6}	0.99	0.99 ± 0.004	$0.99 \pm 6.9 \times 10^{-4}$	1.0
HAP F127	10,799 ± 713	9.28×10^{-6}	1.00	0.99 ± 0.003	$0.99 \pm 5.4 \times 10^{-4}$	1.0

The maximal adsorption capacities for HAP, HAP P123, and HAP F127 were 11,071, 11,035, and 10,799 mg/g, respectively. Both models showed high R^2 values. However, the AIC test indicated that the Freundlich model was more appropriate for describing experimental data. According to the Langmuir model, the homogeneous reaction was mainly responsible for indium ion adsorption [42]. The Freundlich model, on the other hand, addresses equilibrium on a heterogeneous surface [6]. Thus, indium adsorption onto HAP and its two modifications can be considered as a complex physico-chemical process and homogeneous and heterogeneous levels that have played a role in sorption [41]. The R_L value for all adsorbents was lower than 1.0 (0.5–0.9), indicating favorable adsorption.

The literature's values for other sorbents were compared with the adsorption capacities of HAP and its two modifications (Table 3). As can be seen from the table, high sorption capacities were reported for mesoporous silica [10], titanosilicate [10], and supercritical-modified chitin [21], whereas low adsorption capacities were reported for phosphorylated sawdust [12], solvent-impregnated resins [16], and poly(vinylphosphonic acid-*co*-acrylic acid) nanobeads[6], respectively. For the studied sorbents, the adsorption capacity was the highest among the reported data, showing that HAP had an extraordinary affinity toward indium ions.

3.4. Effect of Temperature on Indium Removal by HAP Adsorbents and Thermodynamics of the Study

Experiments were conducted at temperatures of 20, 30, 40, and 50 °C to evaluate the impact of temperature on the adsorption capacity (Figure 8). Indium adsorption was discovered to not be temperature-dependent. The removal efficiency of HAP and its modifications was on the level of 96–99%.

Table 3. The comparison of maximum adsorption capacity of indium ions onto different adsorbents.

Adsorbent	Conditions/Kinetic	q, mg/g	References
HAP	pH = 4, t = 22 °C/PSO	11,071	Present study
HAP P123	pH = 5, t = 22 °C/PSO	11,035	Present study
HAP F127	pH = 4, t = 22 °C/PSO	10,799	Present study
Poly(vinylphosphonic acid-*co*-acrylic acid) nanobeads	pH = 8, t = 25 °C	59.71	[6]
Mesoporous silica SBA-15	pH = 6, t = 22 °C/PSO	2267	[10]
Titanosilicate ETS-10	pH = 3, t = 22 °C/PSO	367	[10]
Powdered phosphorylated sawdust	pH = 3.5	1.121	[12]
Solvent-impregnated resins	t = 25 °C/PSO	29.45	[16]
Ion Imprinted Polymer	t = 25 °C/PSO	60.62	[17]
Supercritical modified chitin	t = 25 °C/PSO	137.69	[21]
SiO_2@GO-PO_3H_2	pH = 3, t = 25 °C/PSO	149.83	[23]
Poly (melamine-formic acid) network	pH = 4, t = 30 °C/PSO	206.3	[46]
Mesoporous activated carbon	pH = 3.5, t = 25 °C/PSO	9.81	[47]

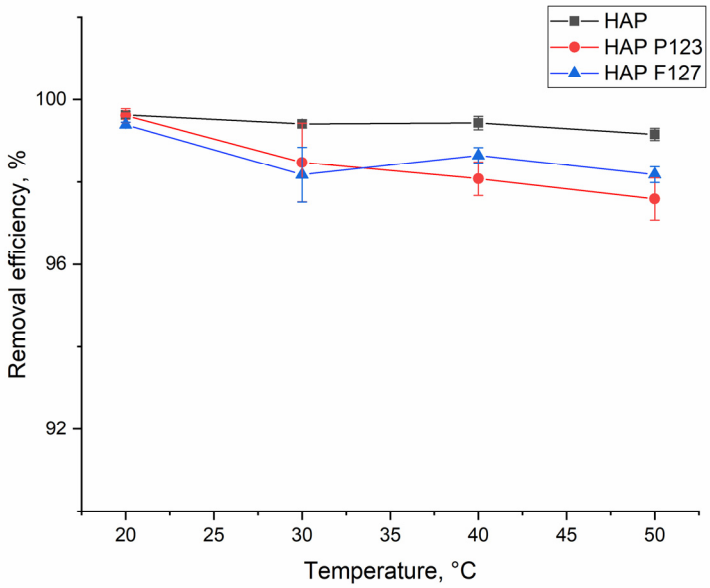

Figure 8. Effect of temperature on indium removal by HAP adsorbents.

By understanding the enthalpy and entropy of adsorption, which were discovered from the slope and intercept of a plot of log ($\ln K_d$) vs. 1/T (Figure S1), the values of Gibbs free energy were determined. Equations (9) and (10) were used to estimate the thermodynamic parameters, including the standard free energy ($\Delta G°$), enthalpy change ($\Delta H°$), and entropy change ($\Delta S°$):

$$\ln K_d = \frac{\Delta S^0}{R} - \frac{\Delta H^0}{RT} \quad (9)$$

$$\Delta G^0 = \Delta H^0 - T\Delta S^0 \quad (10)$$

The distribution coefficient K_d was calculated using Equation (11):

$$K_d = \frac{C_a}{C_e} \quad (11)$$

where C_a is the concentration of indium(III) adsorbed, mg/L.

The thermodynamic parameters are listed in Table 4.

Table 4. Thermodynamic parameters for indium adsorption at different temperatures.

Sorbent	Temperature, K	ΔG°, kJ/mol	ΔH°, kJ/mol	ΔS°, J/mol·K
HAP	293	−13.5	−19.0	−18.7
	303	−13.3		
	313	−13.1		
	323	−12.9		
HAP P123	293	−12.7	−46.1	−113.8
	303	−11.6		
	313	−10.5		
	323	−9.3		
HAP F127	293	−11.7	−24.1	−42.1
	303	−11.3		
	313	−10.9		
	323	−10.4		

The negative values of Gibbs free energy at the various temperatures show the spontaneous nature of the adsorption process. The negative enthalpy values confirm the exothermic character of the adsorption, while the negative value of entropy suggests decreased randomness during adsorption [42]. The process of indium removal is physical, since ΔH° values were less than 40 KJ/mol [48].

3.5. Effect of Co-Existing Ions on Indium Removal by HAP Adsorbents

In the literature, the process of indium removal from single-metal solutions has mainly been studied [4–6,11]. However, metal ions present in wastewater may compete with indium ions during the adsorption process. Since indium in nature is mainly associated with cadmium, zinc, copper, and tin deposits [5,8], the effect of these metal ions on the efficiency of indium removal was assessed (Figure 9).

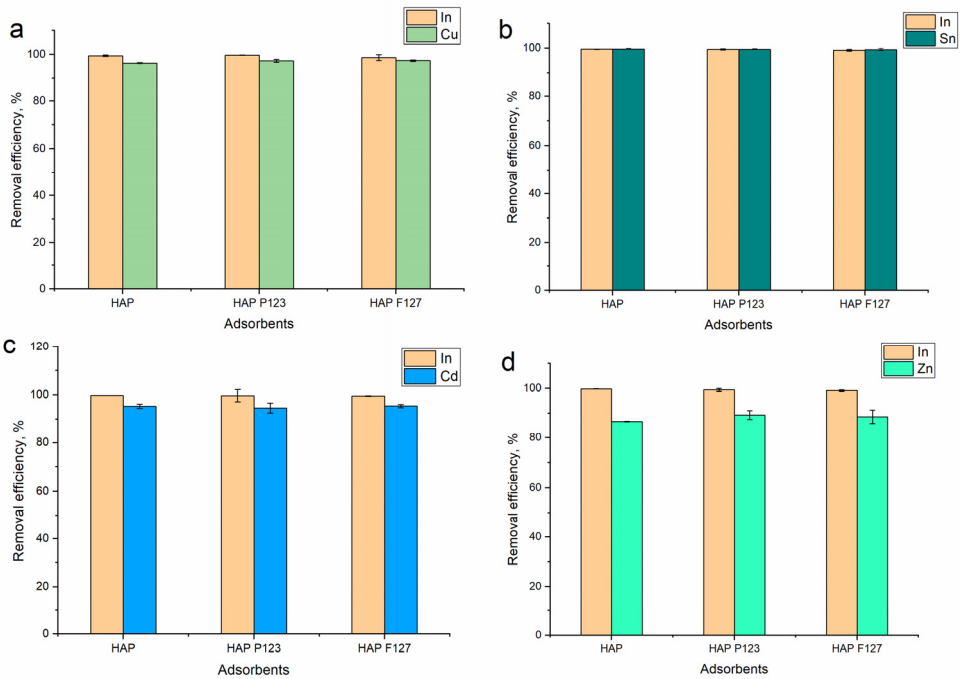

Figure 9. Effect of co-existing ions on indium removal by HAP adsorbents: (**a**) In-Cu system, (**b**) In-Sn system, (**c**) In-Cd system, and (**d**) In-Zn system.

In all analyzed systems, the removal of indium by HAP and its modifications was on the level of 98–99%. Thus, cadmium, zinc, copper, and tin ions had no effect on indium ion removal. The removal of copper was on the level of 96–97%, that of tin was 99%, that of cadmium was 95–96%, and that of zinc was 86–89%. Thus, HAP adsorbents exhibited high adsorption capacities to various metal ions and can be applied for complex wastewater treatment.

Magnesium and aluminum ions did not disturb the adsorption of indium onto UiO-66 [35]. Indium adsorption was inhibited in the presence of iron in the solution [37].

3.6. Adsorbents' Reusability

High stability and the possibility for multiple uses are crucial factors in the choosing of sorbents for the removal of pollutants from wastewaters. It was established that using 0.01 M HCl as an eluent with a high efficiency of indium desorption for all adsorbents can be attained (Figure 10). During three cycles, the desorption efficiency of HAP decreased from 99.4 to 95.4%, that of HAP P123 from 99 to 95.8%, and that of HAP F127 from 99.5 to 96.1%.

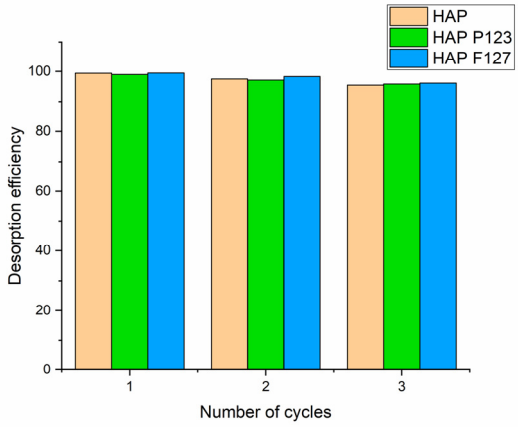

Figure 10. Desorption efficiency of the studied adsorbents during three cycles.

3.7. Theoretical Modeling

The interaction between the structure containing indium and the adsorbent layer (HAP) was also investigated using theoretical chemistry methods. Thus, the density functional theory, DFT [49], with the def2 double-zeta basis set and Becke three-parameter exchange and Lee–Yang–Parr correlation (B3LYP) [50] from the ORCA quantum software package [51] was used. A small fragment of hexagonally crystallized hydroxyapatite, to represent the adsorbent layer, and a pentahydrate structure for the indium sulfate were considered.

The spatial geometry of pentahydrated indium sulfate, considered to be obtained from $In_2(SO_4)_3$, was studied in the gaseous phase and in the aqueous phase. An ideal octahedron configuration for the indium (III) atom in the gas phase with a distance of 3.14 Å between In and the S atom and 2.16 Å between the central atom and the water molecules was considered (Figure 11a). We observed the existence of two hydrogen-bond-type interactions between two water molecules in the equatorial plane of the configuration with two oxygen atoms from the sulfate group. As a result of the optimization of the molecular geometry (in the gaseous phase, but also in the aqueous phase), a proton of a water molecule involved in hydrogen bond interactions was transferred to the sulfate group, resulting in an In-OH covalent bond, approximately 2 Å (Figure 11b). This structure was more stable by approximately 36.5 kcal/mol in the gaseous phase, respectively, and by 8.2 kcal/mol in the aqueous phase, compared with the initial structure, and was considered in the study of adsorption on the macrostructure. The length of the distances between the indium atom and the water molecules increased to 2.28 Å, 2.22 Å for the molecule involved

in a hydrogen bond interaction with an oxygen atom of the sulfate group. The volume of the indium structure was calculated to be 1442.88 Å3.

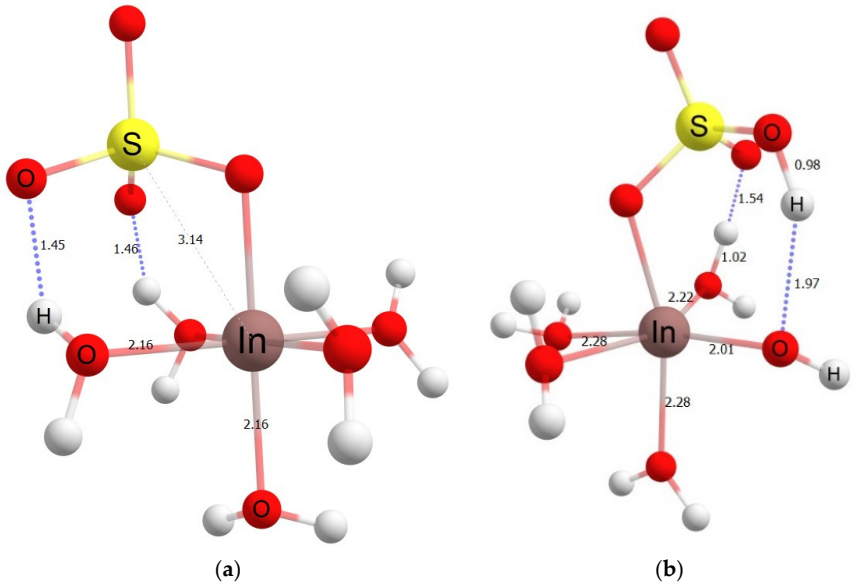

Figure 11. The spatial structure of pentahydrated indium sulfate: (**a**) the initial, ideal, octahedron configuration of the indium atom, (**b**) the optimized geometry. Distances represented are in Å.

The interaction of the hydrated indium sulfate molecule with hydroxyapatite took place on the surface or inside the cavities of the macrostructure through the formation of hydrogen bonds. The sulfate part of the molecule interacted through the hydroxyl group with a similar function in hydroxyapatite, resulting in two hydrogen bonds and, thus, fixing the group to a Ca atom in the substrate. The molecular part containing indium interacted through the water molecules that surrounded it with the oxygen atoms from the PO4 group in the HAP composition, resulting in hydrogen bonds that "anchor" the configuration to it (Figure 12). Thus, the indium structure was retained, adsorbed on the surface or in the cavities of the macrosubstrate. The desorption can be performed using an acidic environment, which will cause the formation of hydrogen bonds competing with those that fix the indium sulfate on the surface of the hydroxyapatite.

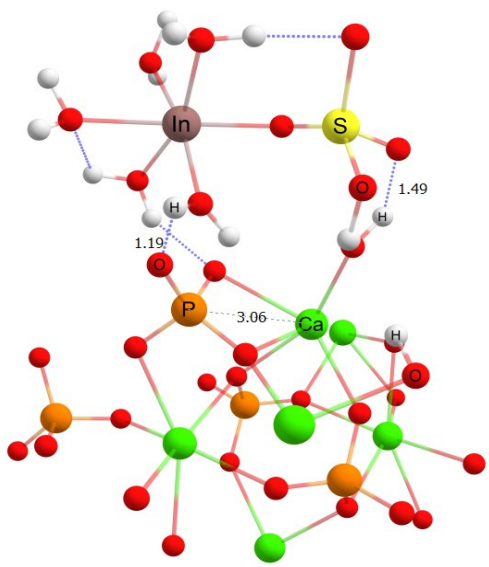

Figure 12. Illustration of the hydrogen bonds and the retention of the indium structure on the surface, or cavities, of the HAP macrostructure (distances are expressed in angstroms).

4. Conclusions

The excellent adsorption capacity of hydroxyapatite and its two modifications, HAP P123 and HAP F127, was attained. The adsorption's optimum pH was found to be 4.0 for all adsorbents and equilibrium was reached in 15 to 45 min. Equilibrium experimental data were well-explained by the Freundlich model, while the maximum adsorption capacity estimated using the Langmuir model ranged from 10,799 mg/g for HAP F127 to 11,071 mg/g for HAP. The kinetics of the adsorption process followed the pseudo-second-order model for HAP, the pseudo-first-order model for HAP P123, and the Elovich model for HAP F127. The indium adsorption process was exothermic, irreversible, and spontaneous from a thermodynamic perspective. Copper, cadmium, tin, and zinc did not interfere with the removal of indium. The studied adsorbents can be applied for multiple wastewater treatments, demonstrating high adsorption and desorption capacity during three cycles. FTIR analysis and theoretical calculations showed that the mechanism of indium adsorption involves ion-exchange with calcium ions and metal ions binding to OH and PO_4^{3-} groups. Hydroxyapatite and its two modifications can be efficiently applied for the treatment of real indium-containing effluents. Due to the high adsorption capacity of HAP, in cases of indium-containing effluents its modification is not necessarily required.

Supplementary Materials: The following supporting information can be downloaded at: https://www.mdpi.com/article/10.3390/separations10070401/s1, Figure S1: $\ln K_d$ vs. 1/T.

Author Contributions: Conceptualization, I.Z. and N.Y.; methodology, I.Z. and D.H.; validation, N.Y., D.G. and I.H.; investigation, I.Z., N.Y., D.H., M.I., D.G. and I.H.; XRD analysis, T.V.; writing—original draft preparation, I.Z. and D.H.; writing—review and editing, all authors; visualization, I.Z. and N.Y. All authors have read and agreed to the published version of the manuscript.

Funding: This research received no external funding.

Data Availability Statement: All data are presented in the manuscript.

Conflicts of Interest: The authors declare no conflict of interest.

References

1. Varghese, A.G.; Paul, S.A.; Latha, M.S. Remediation of Heavy Metals and Dyes from Wastewater Using Cellulose-Based Adsorbents. *Environ. Chem. Lett.* **2019**, *17*, 867–877. [CrossRef]
2. Swain, B.; Mishra, C.; Hong, H.S.; Cho, S.S. Selective Recovery of Pure Copper Nanopowder from Indium-Tin-Oxide Etching Wastewater by Various Wet Chemical Reduction Process: Understanding Their Chemistry and Comparisons of Sustainable Valorization Processes. *Environ. Res.* **2016**, *147*, 249–258. [CrossRef] [PubMed]
3. Jaishankar, M.; Tseten, T.; Anbalagan, N.; Mathew, B.B.; Beeregowda, K.N. Toxicity, Mechanism and Health Effects of Some Heavy Metals. *Interdiscip. Toxicol.* **2014**, *7*, 60–72. [CrossRef]
4. Wei, S.; Liu, J.; Zhang, S.; Chen, X.; Liu, Q.; Zhu, L.; Guo, L.; Liu, X. Stoichiometry, Isotherms and Kinetics of Adsorption of In(III) on Cyanex 923 Impregnated HZ830 Resin from Hydrochloric Acid Solutions. *Hydrometallurgy* **2016**, *164*, 219–227. [CrossRef]
5. Kwak, N.S.; Baek, Y.; Hwang, T.S. The Synthesis of Poly(Vinylphosphonic Acid-Co-Methacrylic Acid) Microbeads by Suspension Polymerization and the Characterization of Their Indium Adsorption Properties. *J. Hazard. Mater.* **2012**, *203–204*, 213–220. [CrossRef] [PubMed]
6. Kwak, N.S.; Park, H.M.; Hwang, T.S. Preparation of Ion-Exchangeable Nanobeads Using Suspension Polymerization and Their Sorption Properties for Indium in Aqueous Solution. *Chem. Eng. J.* **2012**, *191*, 579–587. [CrossRef]
7. Yang, J.; Retegan, T.; Ekberg, C. Indium Recovery from Discarded LCD Panel Glass by Solvent Extraction. *Hydrometallurgy* **2013**, *137*, 68–77. [CrossRef]
8. Xu, S.; Wang, G.; Fan, J.; Wang, Z.; Zhang, J.; Chen, J.; Zheng, L.; Pan, J.; Wang, R. Preparation of High Purity Indium by Chemical Purification: Focus on Removal of Cd, Pb, Sn and Removal Mechanism. *Hydrometallurgy* **2021**, *200*, 105551. [CrossRef]
9. Medvecký, L.; Briančin, J. Possibilities of Simultaneous Determination of Indium and Gallium in Binary InGa Alloys by Anodic Stripping Voltammetry in Acetate Buffer. *Chem. Pap.* **2004**, *58*, 93–100.
10. Zinicovscaia, I.; Yushin, N.; Humelnicu, D.; Grozdov, D.; Ignat, M.; Humelnicu, I. Adsorption Capacity of Silica SBA-15 and Titanosilicate ETS-10 toward Indium Ions. *Materials* **2023**, *16*, 3201. [CrossRef]
11. Hwang, C.W.; Kwak, N.S.; Hwang, T.S. Preparation of Poly(GMA-Co-PEGDA) Microbeads Modified with Iminodiacetic Acid and Their Indium Adsorption Properties. *Chem. Eng. J.* **2013**, *226*, 79–86. [CrossRef]
12. Jeon, C.; Cha, J.H.; Choi, J.Y. Adsorption and Recovery Characteristics of Phosphorylated Sawdust Bead for Indium (III) in Industrial Wastewater. *J. Ind. Eng. Chem.* **2015**, *27*, 201–206. [CrossRef]

13. Calagui, M.J.C.; Senoro, D.B.; Kan, C.C.; Salvacion, J.W.L.; Futalan, C.M.; Wan, M.W. Adsorption of Indium (III) Ions from Aqueous Solution Using Chitosan-Coated Bentonite Beads. *J. Hazard. Mater.* **2014**, *277*, 120–126. [CrossRef] [PubMed]
14. Zhang, D.; Zhang, Y.; Lu, W.; Le, X.; Li, P.; Huang, L.; Zhang, J.; Yang, J.; Serpe, M.J.; Chen, D.; et al. Fluorescent Hydrogel-Coated Paper/Textile as Flexible Chemosensor for Visual and Wearable Mercury (II) Detection. *Adv. Mater. Technol.* **2019**, *4*, 1800201. [CrossRef]
15. Zhang, D.; Yao, Y.; Wu, J.; Protsak, I.; Lu, W.; He, X.; Xiao, S.; Zhong, M.; Chen, T.; Yang, J. Super Hydrophilic Semi-IPN Fluorescent Poly(N-(2-Hydroxyethyl)Acrylamide) Hydrogel for Ultrafast, Selective, and Long-Term Effective Mercury (II) Detection in a Bacteria-Laden System. *ACS Appl. Bio Mater.* **2019**, *2*, 906–915. [CrossRef]
16. Li, H.; Liu, J.; Gao, X.; Liu, C.; Guo, L.; Zhang, S.; Liu, X.; Liu, C. Adsorption Behavior of Indium (III) on Modified Solvent Impregnated Resins (MSIRs) Containing Sec-Octylphenoxy Acetic Acid. *Hydrometallurgy* **2012**, *121–124*, 60–67. [CrossRef]
17. Li, M.; Meng, X.; Liang, X.; Yuan, J.; Hu, X.; Wu, Z.; Yuan, X. A Novel In(III) Ion-Imprinted Polymer (IIP) for Selective Extraction of In(III) Ions from Aqueous Solutions. *Hydrometallurgy* **2018**, *176*, 243–252. [CrossRef]
18. Alguacil, F.J.; Lopez, F.A.; Rodriguez, O.; Martinez-Ramirez, S.; Garcia-Diaz, I. Sorption of Indium (III) onto Carbon Nanotubes. *Ecotoxicol. Environ. Saf.* **2016**, *130*, 81–86. [CrossRef]
19. Huang, C.C.; Huang, J.J. Adsorption of Indium and Zinc Ions from Aqueous Solutions by Carboxymethyl Chitosan/Poly(Acrylic Acid) Microbeads. *Desalin. Water Treat.* **2018**, *118*, 230–240. [CrossRef]
20. Homhuan, N.; Bureekaew, S.; Ogawa, M. Efficient Concentration of Indium (III) from Aqueous Solution Using Layered Silicates. *Langmuir* **2017**, *33*, 9558–9564. [CrossRef]
21. Li, Z.; Dotto, G.L.; Bajahzar, A.; Sellaoui, L.; Belmabrouk, H.; Ben Lamine, A.; Bonilla-Petriciolet, A. Adsorption of Indium (III) from Aqueous Solution on Raw, Ultrasound- and Supercritical-Modified Chitin: Experimental and Theoretical Analysis. *Chem. Eng. J.* **2019**, *373*, 1247–1253. [CrossRef]
22. Roosen, J.; Mullens, S.; Binnemans, K. Multifunctional Alginate-Sulfonate-Silica Sphere-Shaped Adsorbent Particles for the Recovery of Indium (III) from Secondary Resources. *Ind. Eng. Chem. Res.* **2017**, *56*, 8677–8688. [CrossRef]
23. Li, M.; Meng, X.; Huang, K.; Feng, J.; Jiang, S. A Novel Composite Adsorbent for the Separation and Recovery of Indium from Aqueous Solutions. *Hydrometallurgy* **2019**, *186*, 73–82. [CrossRef]
24. Aissa, A.; Othmani, M. Heavy Metals Removal Using Nano-Hydroxyapatite Extracted from Cattle Bones. *ChemistrySelect* **2023**, *8*, e202300165. [CrossRef]
25. Nayak, A.; Bhushan, B. Hydroxyapatite as an Advanced Adsorbent for Removal of Heavy Metal Ions from Water: Focus on Its Applications and Limitations. In Proceedings of the Materials Today: Proceedings; Elsevier: Amsterdam, The Netherlands, 2021; Volume 46, pp. 11029–11034.
26. Andrew Ofudje, E.; Sodiya, E.F.; Olanrele, O.S.; Akinwunmi, F. Adsorption of Cd^{2+} onto Apatite Surface: Equilibrium, Kinetics and Thermodynamic Studies. *Heliyon* **2023**, *9*, e12971. [CrossRef] [PubMed]
27. Yan, Y.; Du, M.; Jing, L.; Zhang, X.; Li, Q.; Yang, J. Green Synthesized Hydroxyapatite for Efficient Immobilization of Cadmium in Weakly Alkaline Environment. *Environ. Res.* **2023**, *223*. [CrossRef]
28. Núñez, D.; Serrano, J.A.; Mancisidor, A.; Elgueta, E.; Varaprasad, K.; Oyarzún, P.; Cáceres, R.; Ide, W.; Rivas, B.L. Heavy Metal Removal from Aqueous Systems Using Hydroxyapatite Nanocrystals Derived from Clam Shells. *RSC Adv.* **2019**, *9*, 22883–22890. [CrossRef]
29. Zinicovscaia, I.; Yushin, N.; Abdusamadzoda, D.; Grozdov, D.; Humelnicu, I.; Ignat, M.; Humelnicu, D. Removal of Vanadium Ions from Aqueous Solutions Using Different Type of Hydroxyapatites: Adsorption Isotherm, Kinetics and Thermodynamic Studies. *Environ. Eng. Manag. J.* **2021**, *20*, 871–881. [CrossRef]
30. Zinicovscaia, I.; Yushin, N.; Grozdov, D.; Humelnicu, I.; Humelnicu, D.; Mitina, T. Removal of Chromium (III) Ions from Aqueous Solutions Using Different Types of Hydroxyapatites. *Desalin. Water Treat.* **2020**, *204*, 297–305. [CrossRef]
31. Arsad, M.S.M.; Lee, P.M. Synthesis and Characterization of Hydroxyapatite Nanoparticles and β-TCP Particles. *2nd Int. Conf. Biotechnol. Food Sci.* **2011**, *7*, 184–188.
32. Mohammad, N.F.; Othman, R.; YEOH, F.Y. Controlling the Pore Characteristics of Mesoporous Apatite Materials: Hydroxyapatite and Carbonate Apatite. *Ceram. Int.* **2015**, *41*, 10624–10633. [CrossRef]
33. Sheha, R.R. Sorption Behavior of Zn (II) Ions on Synthesized Hydroxyapatites. *J. Colloid Interface Sci.* **2007**, *310*, 18–26. [CrossRef] [PubMed]
34. Sairam Sundaram, C.; Viswanathan, N.; Meenakshi, S. Fluoride Sorption by Nano-Hydroxyapatite/Chitin Composite. *J. Hazard. Mater.* **2009**, *172*, 147–151. [CrossRef] [PubMed]
35. Zeng, W.; Xu, L.; Wang, Q.; Chen, C.; Fu, M. Adsorption of Indium (III) Ions from an Acidic Solution by Using UiO-66. *Metals* **2022**, *12*, 579. [CrossRef]
36. Chou, W.L.; Wang, C.T.; Huang, K.Y.; Chang, Y.C.; Shu, C.M. Investigation of Indium Ions Removal from Aqueous Solutions Using Spent Coffee Grounds. *Int. J. Phys. Sci.* **2012**, *7*, 2445–2454. [CrossRef]
37. Pennesi, C.; Amato, A.; Occhialini, S.; Critchley, A.T.; Totti, C.; Giorgini, E.; Conti, C.; Beolchini, F. Adsorption of Indium by Waste Biomass of Brown Alga Ascophyllum Nodosum. *Sci. Rep.* **2019**, *9*, 16763. [CrossRef]
38. Xiong, C.H.; Lu, B.W.; Wang, Y.J. Sorption Behavior and Mechanism of Indium (III) onto Amino Methylene Phosphonic Acid Resin. *J. Wuhan Univ. Technol. Mater. Sci. Ed.* **2002**, *17*, 47–50. [CrossRef]

39. El-Shazly, E.A.A.; Moussa, S.I.; Dakroury, G.A. Recovery of Some Rare-Earth Elements by Sorption Technique onto Graphene Oxide. *J. Sustain. Metall.* **2022**, *8*, 715–731. [CrossRef]
40. Jiang, J.; Long, Y.; Hu, X.; Hu, J.; Zhu, M.; Zhou, S. A Facile Microwave-Assisted Synthesis of Mesoporous Hydroxyapatite as an Efficient Adsorbent for Pb^{2+} Adsorption. *J. Solid. State Chem.* **2020**, *289*, 121491. [CrossRef]
41. Billah, R.E.K.; Khan, M.A.; Park, Y.K.; Am, A.; Majdoubi, H.; Haddaji, Y.; Jeon, B.H. A Comparative Study on Hexavalent Chromium Adsorption onto Chitosan and Chitosan-Based Composites. *Polymers* **2021**, *13*, 3427. [CrossRef]
42. Sen, T.K.; Gomez, D. Adsorption of Zinc (Zn^{2+}) from Aqueous Solution on Natural Bentonite. *Desalination* **2011**, *267*, 286–294. [CrossRef]
43. Wakamura, M.; Kandori, K.; Ishikawa, T. Surface Composition of Calcium Hydroxyapatite Modified with Metal Ions. *Colloids Surf. A Physicochem. Eng. Asp.* **1998**, *142*, 107–116. [CrossRef]
44. El-Maghrabi, H.H.; Younes, A.A.; Salem, A.R.; Rabie, K.; El-shereafy, E. Magnetically Modified Hydroxyapatite Nanoparticles for the Removal of Uranium (VI): Preparation, Characterization and Adsorption Optimization. *J. Hazard. Mater.* **2019**, *378*, 120703. [CrossRef] [PubMed]
45. Aydin, H.; Bulut, Y.; Yerlikaya, Ç. Removal of Copper (II) from Aqueous Solution by Adsorption onto Low-Cost Adsorbents. *J. Environ. Manag.* **2008**, *87*, 37–45. [CrossRef]
46. Li, G.; Zhang, B.; Ma, Z.; Wang, Z. Facile Synthesis of Hydroxyl- and Amine-Riched Porous Polymer for Indium Recovery in Water. *Microporous Mesoporous Mater.* **2021**, *323*, 111162. [CrossRef]
47. Díez, E.; Gómez, J.M.; Rodríguez, A.; Bernabé, I.; Sáez, P.; Galán, J. A New Mesoporous Activated Carbon as Potential Adsorbent for Effective Indium Removal from Aqueous Solutions. *Microporous Mesoporous Mater.* **2020**, *295*. [CrossRef]
48. Sepehri, S.; Kanani, E.; Abdoli, S.; Rajput, V.D.; Minkina, T.; Asgari Lajayer, B. Pb (II) Removal from Aqueous Solutions by Adsorption on Stabilized Zero-Valent Iron Nanoparticles—A Green Approach. *Water* **2023**, *15*, 222. [CrossRef]
49. Kohn, W.; Becke, A.D.; Parr, R.G. Density Functional Theory of Electronic Structure. *J. Phys. Chem.* **1996**, *100*, 12974–12980. [CrossRef]
50. Neese, F. The ORCA Program System. *Wiley Interdiscip. Rev. Comput. Mol. Sci.* **2012**, *2*, 73–78. [CrossRef]
51. Becke, A.D. A New Mixing of Hartree-Fock and Local Density-Functional Theories. *JChPh* **1993**, *98*, 1372–1377. [CrossRef]